Modeling Cultural Segregation of the Queer Community Through an Adaptive Social Network Model

Heijmans, Pieke; van Stijn, Jip; Treur, Jan

published in
Fourth International Congress on Information and Communication Technology
2020

DOI (link to publisher)
10.1007/978-981-32-9343-4_19

document version
Publisher's PDF, also known as Version of record

Modeling Cultural Segregation of the Queer Community Through an Adaptive Social Network Model

Pieke Heijmans, Jip van Stijn and Jan Treur

Abstract In this study, the forming of social communities and segregation is examined through a case study on the involvement in the queer community. This is examined using a temporal-causal network model. In this study, several scenarios are proposed to model this segregation and a small questionnaire is set up to collect empirical data to validate the model. Mathematical verification provides insight into the model's expected behavior.

Keywords Queer community · Temporal-causal network · Social hardship · Social contagion · Homophily principle · Social network · Cultural segregation

1 Introduction

In a developed world that contains increasingly pluralistic and diverse societies, the establishment of subcultures seems inevitable. In the West, subcultures are associated with an increased identification with in-group individuals, leading to a caring environment. However, subcultures are at risk of a high degree of segregation and misunderstanding of and by out-group individuals, possibly leading to discrimination and aggression. In view of stimulating and maintaining peaceful and democratic processes in these societies, it can be useful to investigate this behavior. This can be performed through network-oriented modeling, which describes the behaviors and opinions of people in relation to the connections among them. In graphical representations of social networks, individuals and their states are depicted by nodes which are connected by uni- or bidirectional links.

P. Heijmans (✉) · J. van Stijn · J. Treur
Behavioural Informatics Group, Vrije Universiteit Amsterdam, Amsterdam, The Netherlands
e-mail: piekeheijmans@gmail.com

J. van Stijn
e-mail: jipvanstijn@gmail.com

J. Treur
e-mail: j.treur@vu.nl

X.-S. Yang et al. (eds.), *Fourth International Congress on Information and Communication Technology*, Advances in Intelligent Systems and Computing 1027, https://doi.org/10.1007/978-981-32-9343-4_19

In this paper, firstly some background about cultural segregation of the queer community is discussed. Next, the network model is explained including the homophily and social contagion principle. In addition, some different scenarios for the model are set up and different simulations with the model are discussed. It will be shown how mathematical verification clarifies how different parameters influence the outcomes of the model. The current paper investigates subculture identification and cultural segregation of the queer community. Being born differently from the heteronormative society that they grow up in, queer people have to deal with a number of factors that contribute to a permanent level of distress. Meyer [9] frames this psychological distress as minority stress. Due to a continuous internalized homophobia, stigma, which relates to society's expectations, and experiencing actual discrimination or violence, minority stress is established. She found a strong connection between experiencing minority stress and dealing with psychological distress. She adds that hiding and concealing, expectation of rejection, and ameliorative coping processes contribute to this psychological minority stress as well [10].

To deal with psychological distress, a social support system can help. For example, successful coming-out stories of other queer people can help reduce the anxiety of getting negative reactions from friends and family. Wright and Perry claim that support systems are necessary as they influence the development of young people's self-concept and self-esteem [10]. Queer community and queer community spaces can function as this social support system. Beemyn [2] examines the historical role of queer spaces and states that queer people needed their own space, not only to escape from governmental pressures such as police harassment, but also to not deal with constant territorial struggle, a place where they could escape the dominant cultural order. These processes lead to cultural segregation, as consequently queers will distantiate themselves from the dominant cultural order by collectively grouping together in their own communities. Another strong reason to get involved in such a community is collectivism, in the sense that people want to benefit their group. The more you are involved with and identify with this subgroup, the greater your sense of collectivism [1], and thus, the stronger the effect of cultural segregation will be.

From these theories, we expect queer people with a greater experience of hardship and psychological distress to get involved more in the queer community as the community serves as a support system, resulting in a stronger cultural segregation. In contrast, queer people that experience no to little hardship are not inclined to look for a social support system; however, they may be involved with the community for other reasons, for example, relating to their peers. Finally, straight people that experience hardship may look for community support, but not necessarily for the queer community as they do not particularly identify with this group and do not have a strong sense of collectivism. Resulting from these conclusions, it can be expected that a certain group of queer people will get involved with their community, finding comfort, support, and finding equals. In contrast, straight people will not share these needs and will not identify strongly with the queer community. The result is cultural segregation, in which queer people's identification with their community is opposed to straight people's identification.

These processes were analyzed computationally by designing an adaptive network model based on the homophily principle that describes bonding between persons that consider each other similar in some respect(s); see, for example, [8]. This principle works in combination with the principle of social contagion [3] in a circular mutual causal relationship, also called co-evolution [5, 18]. In Sect. 2, the adaptive temporal-causal network model based on these two principles is introduced. Section 3 illustrates the model by example simulations. In Sect. 4, it is shown that the simulation outcomes are in accordance with what is predicted by a mathematical analysis of the model. Section 5 describes validation of the model by comparing simulation outcomes to empirical data and applies parameter tuning. Finally, Sect. 6 is a conclusion.

2 The Adaptive Temporal-Causal Network Model

Thus, the following difference and differential equation for state Y are obtained:A network-oriented modeling approach based on temporal-causal networks [13, 14, 17] was used to analyze the type of processes described in Sect. 1. This approach can be considered as a branch in the causal modeling area which has a long tradition in AI; e.g., see [6, 7, 11]. It distinguishes itself by a dynamic perspective on causal relations, according to which causal relations exert causal effects over time, and these causal relations themselves can also change over time. The type of network models that form the basis is called a *temporal-causal network model*. These network models can be used to translate informally described theories from a variety of human-directed disciplines into adaptive and dynamical numerical models. It takes into account states and their causal effects on other states. The strengths of causal relations from a state X to a state Y are indicated by differences in connection weights $\boldsymbol{\omega}_{X,Y}$. These connection weights can be combined with activation levels $Y(t)$ of states Y and used as input for combination functions $\mathbf{c}_Y(\ldots)$ to determine the aggregated impacts on the states. The precise dynamics of the network are also defined using speed factors $\boldsymbol{\eta}_Y$ of states Y. The network becomes adaptive when connection weights are dynamic as well. The conceptual representation basically is a graph of states and their causal relations; a graphical overview of the network is represented as depicted in Fig. 2. The numerical representation is a translation of this conceptual representation in the way described in Table 1.

$$\begin{aligned} Y(t+\Delta t) &= Y(t) + \boldsymbol{\eta}_Y\big[\mathrm{c}_Y\big(\boldsymbol{\omega}_{X_1,Y}X_1(t),\ldots,\boldsymbol{\omega}_{X_k,Y}X_k(t)\big) - Y(t)\big]\Delta t \\ \mathrm{d}Y(t)/\mathrm{d}t &= \boldsymbol{\eta}_Y\big[\mathrm{c}_Y\big(\boldsymbol{\omega}_{X_1,Y}X_1(t),\ldots,\boldsymbol{\omega}_{X_k,Y}X_k(t)\big) - Y(t)\big] \end{aligned} \quad (1)$$

The adaptive social network model used here is based on two fundamental principles. Firstly, the notion of social contagion is used to explain the causal influence of one state on another through the connection between the two [3]. This principle accounts for the change of state values over time, and its numerical representation is (where

Table 1 From conceptual representation to numerical representation of a temporal-causal network model; adopted from [17]

Concept	Representation	Explanation
State values over time t	$Y(t)$	At each time point t, each state Y in the model has a real number value in [0, 1]
Single causal impact	$\mathbf{impact}_{X,Y}(t) = \boldsymbol{\omega}_{X,Y}\, X(t)$	At t, state X with connection to state Y has an impact on Y, using connection weight $\boldsymbol{\omega}_{X,Y}$
Aggregating multiple impacts	$\mathbf{aggimpact}_Y(t)\ {}_Y(\mathbf{impact}_{X1,Y}(t),\ldots, \mathbf{impact}_{Xk,Y}(t)) = \mathbf{c}_Y(\boldsymbol{\omega}_{X1,Y}X_1(t), \ldots, {}_{Xk,Y}X_k(t))$	The aggregated causal impact of multiple states X_i on Y at t is determined using combination function $\mathbf{c}_Y(..)$
Timing of the causal effect	$Y(t+\Delta t) = Y(t) + \boldsymbol{\eta}_Y [\mathbf{aggimpact}_Y(t) - Y(t)]\,\Delta t = Y(t) + \boldsymbol{\eta}_Y [\mathbf{c}_Y(\boldsymbol{\omega}_{X1,Y}X_1(t), \ldots, \boldsymbol{\omega}_{Xk,Y}X_k(t)) - Y(t)]\,\Delta t$	The causal impact on Y is exerted over time gradually, using speed factor $\boldsymbol{\eta}_Y$; here, the X_i are all states with connections to state Y

X_{Ai} and X_B are the states of persons A_i and B):

$$\begin{aligned} \mathrm{d}X_B/\mathrm{d}t &= \boldsymbol{\eta}_B\left[\mathrm{c}_B\left(\boldsymbol{\omega}_{A_1,B}X_{A_1}, \ldots, \boldsymbol{\omega}_{A_k,B}X_{A_k}\right) - X_B\right] \\ X_B(t+\Delta t) &= X_B(t) + \boldsymbol{\eta}_B[\mathrm{c}_B\left(\boldsymbol{\omega}_{A_1,B}X_{A_1}(t), \ldots, \boldsymbol{\omega}_{A_k,B}X_{A_k}(t)\right) - X_B(t)]\Delta t \end{aligned} \quad (2)$$

One option for the combination functions for modeling the aggregated impact of multiple states on another is the scaled sum function:

$$\mathbf{ssum}_\lambda(V_1, \ldots V_k) = (V_1 + \cdots + V_k)/\lambda \quad (3)$$

Usually, a normalized scaled sum is used: The value of λ is the sum of all incoming weights $\boldsymbol{\omega}_{X_i,Y}$. In cases that these connection weights change over time an adaptive version of the scaled sum can be used:

$$\mathbf{adapssum}_\lambda(V_1, \ldots V_k) = (V_1 + \cdots + V_k)/\lambda(t) \quad (4)$$

where $\lambda(t)$ is the sum of all incoming weights $\boldsymbol{\omega}_{X_i,Y}(t)$ at t. This version was used to model social contagion in the work reported here. Another function used for social contagion in this research is the advanced logistic sum function:

$$\mathbf{alogistic}_{\sigma,\tau_{\log}}(V_1, \ldots V_k) = \left[\frac{1}{1+\mathrm{e}^{-\sigma\left(V_1+\cdots+V_k-\tau_{\log}\right)}} - \frac{1}{(1+\mathrm{e}^{\sigma\,\tau_{\log}})}\right] (1+\mathrm{e}^{-\sigma\,\tau_{\log}}) \quad (5)$$

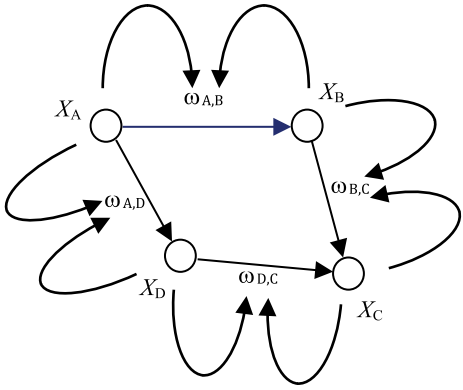

Fig. 1 A conceptual representation of the homophily principle

where σ is the steepness factor and $\tau_{\log}$ the logistic threshold.

Secondly, the principle of homophily describes the change of connection weights between the states X_A and X_B of two persons A and B; e.g., [8]. According to this principle, when the values of two nodes are similar, the connection between them becomes stronger (represented by a higher connection weight). Conversely, the lower the similarity between the (values of) the two nodes, the smaller their connection weight. In Fig. 1, the homophily principle is depicted by the striped arrows. Numerically, this principle can be represented as follows:

$$\begin{aligned} \boldsymbol{\omega}_{A,B}(t+\Delta t) &= \boldsymbol{\omega}_{A,B}(t) + \boldsymbol{\eta}_{A,B}[\mathrm{c}_{A,B}(X_A(t), X_B(t), \boldsymbol{\omega}_{A,B}(t)) - \boldsymbol{\omega}_{A,B}(t)]\,\Delta t \\ \mathrm{d}\boldsymbol{\omega}_{A,B}/\mathrm{d}t &= \boldsymbol{\eta}_{A,B}[\mathrm{c}_{A,B}(X_A, X_B, \boldsymbol{\omega}_{A,B}) - \boldsymbol{\omega}_{A,B}] \end{aligned} \tag{6}$$

in which X_A and X_B represent the states of person A and person B.

In the current paper, the combination function $\mathrm{c}_{A,B}(V_1, V_2, W)$ used for the homophily principle is the following:

$$\mathbf{slhom}_{\tau_{\mathrm{hom}},\alpha}(V_1, V_2, W) = W + \alpha\, W(1-W)(\tau_{\mathrm{hom}} - |V_1 - V_2|) \tag{7}$$

3 Simulations of Example Scenarios

In this section, the adaptive network model is described for three scenarios. In the first example Scenario 1 for this model, a social network of 10 nodes is used, consisting of three communities of three or four nodes. Each community contains one node that is the so-called bridge node, which has connections to the two bridge nodes of the other communities. Within the three communities, there is maximal connectedness: All nodes are connected to the other nodes within the community. As the connections represent social interactions, they are all assumed to be bidirectional. All connections

are presumed to be relatively strong, so all connection weights were set initially to 0.8. The state values represent the individual's identification with the queer culture, with 0 being minimal identification and 1 being maximal identification. The initial values of identification with the queer culture are assumed to be spread evenly on the spectrum of 0.1–1, as depicted in Fig. 2. For social contagion, in this scenario the adaptive normalized scaled sum function was used, with a dynamic scaling factor of the sum of all the connection weights per state at that time. Table 2 shows the values used for the parameters. In this scenario, two simulations were carried out using two different state speed factors. The simulation of this model shows a classic example of the interplay of social contagion and homophily; sometimes also called co-evolution [5, 18]. In Scenario 1.1, a speed factor of 0.2 was used for all states, and the three communities all converged to their own equilibrium value. The connection weights of the within-community connections converged to 1, while the weights of the bridge connections converged to 0. This result is illustrated in Fig. 3.

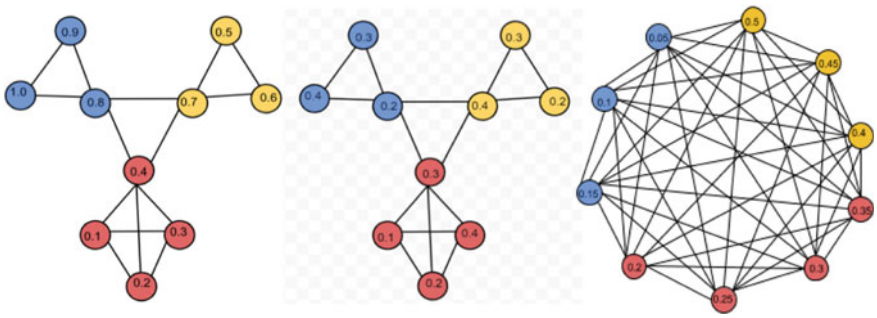

Fig. 2 Left hand: conceptual representation of the network in Scenario 1. Middle: for Scenario 2. Right hand: for scenario 3. Each node represents an individual, with the initial state value illustrated in the node. Each line represents a bidirectional connection. The three communities are labeled with different colors

Table 2 Parameters and their values used in the simulation of Scenarios 1 and 2

Parameters Scenario 1	Values	Parameters Scenarios 2 and 3	Values
State speed factor η_Y	0.2/0.8	State speed factor η_Y	0.2
ω speed factor η_ω	0.5	ω speed factor η_ω	0.5
slhom threshold factor τ_{hom}	0.1	slhom threshold factor τ_{hom}	0.08
slhom amplification factor α	8.0	slhom amplification factor α	8.0
		Alogistic steepness factor σ	2.5
		Alogistic threshold factor τ_{log}	0.18

Except for the initial connection weights mentioned above, all parameters are equal for all states and connections. (ω = connection weight, slhom = simple logistic homophily function, alogistic = advanced logistic function as defined above)

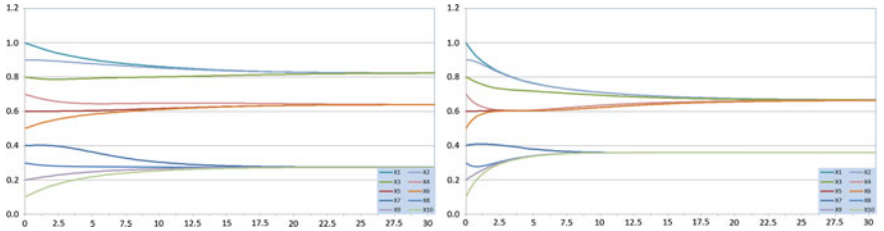

Fig. 3 A graphical representation of the state values in the simulation of Scenarios 1.1 resp. 1.2 for state speed factors 0.2 resp. 0.8. The *y*-axis represents the state values, while the *x*-axis represents time. Every community converges to its own equilibrium value. Social contagion is quicker in Scenario 1.2 than in Scenario 1.1. This leads to the fact that the first two communities converge toward each other. The third community still converges to its own equilibrium

The final example Scenario 3 concerns a fully connected network in which each node is connected to every other node. Figure 5 shows a conceptual representation of this network. Again, the advanced logistic function is used to model social contagion between the nodes, and the simple homophily function alters the connection weights over time. This scenario is somewhat more life-like than the previous examples, as it is reasonable to assume that, in a group of 10 people, every person knows all others to some degree. All initial connection weights are set to 0.8. In Scenario 1.2, when the state speed factor of 0.8 was used, two of the communities first converge within themselves, and then converged to a shared equilibrium state value. The third community converged to its own equilibrium value. The bridge connection between states 3 and 4 now converged to 1 instead of 0. This shows that the effect of the social contagion function is now quicker than in simulation 1.1 and influences the homophily of the connection weights.

Note that in case that no homophily principle is applied but only the social contagion, according to Theorems 3 and 4 in [15] for the so-called strongly connected network using normalized scaled sum combination functions (which are strictly monotonically increasing and scalar-free [15]) all states will converge to the same value, and this value lies between the minimal and maximal initial state value. The emergence of communities is a result of the homophily, and the faster the contagion in comparison with the homophily principle, the lower the number of communities that emerge, as shown here in Fig. 3.

In the example Scenario 2, the number of nodes and their connectedness is equal to the first scenario. However, the initial values range from 0.1 to 0.4 and this time the advanced logistic function is used for social contagion. The results of this scenario shows that, when using the advanced logistic function to model social contagion, the equilibrium values can end up higher or lower than any initial values of the states, in contrast to what holds for normalized scaled sum functions; see [15]. Most of the states converge to an equilibrium of 1 or 0.982, whereas all the initial values lay between 0.1 and 0.4. This may represent a real-life process in which a sentiment is strengthened and amplified beyond its original level, because it is shared with others.

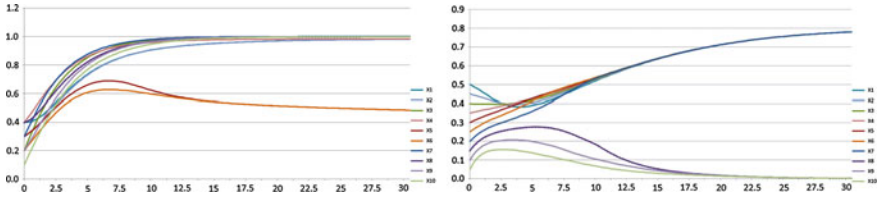

Fig. 4 A graphical representation of the state values in the simulation of Scenarios 2 and 3. The *y*-axis represents the state values, while the *x*-axis represents time. The initial values of all states range between 0.1 and 0.4, while most of the values converge to 1 or 0.982. However, state 4 and 5 converge to 0.415

Yet, the equilibrium values of state 5 and 6 (initial values 0.2 and 0.3) converge to a different, much lower equilibrium of 0.415. The connection weights of all initial connections converge to 1, except for those of state X_4 with X_5 and X_6. This shows that: (1) when using the advanced logistic function in combination with homophily, the initial value of a state does not necessarily determine in which equilibrium it ends up; and (2) that this combination function can strongly influence the connectivity in a network, possibly leading to the change or dissolvement of communities over time. Thus, this simulation demonstrates the phenomenon of segregation within a network (and in a specific community within the network) regardless of a similarity in initial values of the states. Figure 4 shows these results in a graphical representation.

Again, the simulation resulted in the separating behavior into two groups. The seven states with the highest initial values all converge to a value of 0.8, spiraling past their original values. The remaining three states converge to a value of 0.036, well below their initial values. The connection weights within the groups all converge to 1, while the intergroup connections end up with a weight value of 0. This simulation not only shows separating behavior of one group into two communities, as with the previous scenario. It also hints at a notion of extremism, in which the two groups increasingly push each other off. This may be comparable to the process of 'othering', in which the shaping of an identity depends on the supposition with other people's behavior or convictions. This combined with group behavior can then lead to polarization, which can be observed in many social and political situations.

4 Model Verification by Mathematical Analysis

In order to verify the model, first a mathematical analysis of stationary points was performed, in particular for the third scenario. A *stationary point* of a state Y at time t occurs when $\mathrm{d}Y(t)/\mathrm{d}t = 0$. A *stationary point* of a connection weight ω at time t occurs when $\mathrm{d}\omega(t)/\mathrm{d}t = 0$. The network model is in an *equilibrium* at t when all states and all connection weights have a stationary point at t. As described in Sect. 2, in a temporal-causal network model the differential equation for all states is: $\mathrm{d}Y(t)/\mathrm{d}t = \eta_Y$ [**aggimpact**$_Y(t) - Y(t)$]. As all speed factors in the model are nonzero, all

stationary points must follow the criterion: **aggimpact**$_Y(t) = Y(t)$ also formulated as: In a temporal-causal network model, there is a stationary point for state Y at t if and only if $\eta_Y = 0$ or $c_Y(\boldsymbol{\omega}_{X_1,Y}X_1(t), \ldots, \boldsymbol{\omega}_{X_k,Y}X_k(t)) = Y(t)$.

From the modeled data in Scenario 3, stationary points were gathered from several states, and the aggregated impact at that time was calculated per state using the advanced logistic function described earlier. If the state values and the calculated aggregated impact are equal, the stationary point equation above is fulfilled. This mathematically verifies the model. The results are presented in Table 3. As appears in the table, the deviations between the observed state values and the calculated aggregated impact on that state at that time are very low. This indicates that the model does what is expected; it calculates the expected state values with high precision.

When the stationary point Eq. (9) mentioned above applies to all network states and connection weights at a single time, the model is in equilibrium. In the third scenario, the model appears to be in equilibrium at $t = 300$. The state values at this time were read, and the aggregated impact at that moment was calculated per state. The results are presented in Table 4. As is visible in the table, the deviation between the state values and the aggregated impact of all states at $t = 300$ is very low, indicating again that the model calculates the state values in a proper way with high precision.

Additionally, the dynamic connection weights were analyzed. Recall the following combination function for the homophily principle (7):

$$\mathbf{slhom}_{\tau,\alpha}(V_1, V_2, W) = W + \alpha\, W(1 - W)\,(\tau_{\text{hom}} - |V_1 - V_2|) \tag{8}$$

The stationary point criterion of $\mathbf{slhom}\tau_{\text{hom}.\alpha}(V_1, V_2, W) = 0$ provides the equation:

$$W(1 - W)(\tau_{\text{hom}} - |V_1 - V_2|) = W \tag{9}$$

meaning that

$$|V_1 - V_2| = \tau_{\text{hom}} \text{ or } \boldsymbol{\omega}_{A,B} = 0 \text{ or } \boldsymbol{\omega}_{A,B} = 1 \tag{10}$$

Table 3 An overview of stationary point values and the aggregated impact values in the simulation of Scenario 3

State	X_1	X_2	X_3	X_8	X_9	X_{10}
Time point	3.95	3.55	2.10	4.65	3.10	2.55
State value	0.387	0.397	0.397	0.261	0.197	0.145
Aggregated impact	0.388	0.396	0.397	0.262	0.197	0.145
Deviation	0.001	0.001	0	0.001	0	0

States 4–7 did not have a temporary stationary point at the considered time interval. The bottom row shows the deviation between these values

Table 4 State values in the simulation of Scenario 3 at $t = 300$

State	X_1	X_2	X_3	X_4	X_5	X_6	X_7	X_8	X_9	X_{10}
State value	0.802	0.802	0.802	0.802	0.802	0.802	0.802	0.040	0.036	0.038
Agg. impact	0.803	0.802	0.803	0.803	0.802	0.801	0.802	0.038	0.037	0.037
Deviation	0.001	0	0.001	0.001	0	0.001	0	0.002	0.001	0.001

However, the solution $|V_1 - V_2| = \tau_{\text{hom}}$ turns out non-attracting, eliminating this solution as a possible stationary point in the simulation. This corresponds to the connection weight values at $t = 300$ in the simulation of Scenario 3: All connections eventually are either 1 or 0. These connections define the two clusters that appeared, with full connectivity within the communities, and no connection to nodes outside the community.

In a wider context, such an analysis of limit behavior for some classes of homophily combination functions has been presented in [16]. The above analysis fits in that more general approach. In addition to the 0 or 1 values as limit for connection weights, one of the results is that independent of the size of the network there can be at most $1 + 1/\tau_{\text{hom}}$ groups; see [16], Theorem 1a). Indeed, the actual number of the groups in the simulations is less than that predicted maximal number.

5 Validation Using Empirical Data[1]

To validate the proposed model, we acquired a data set for which we set up a questionnaire that participants had to fill out online. The questionnaire consisted of some general introductory questions like age, gender, education, and most importantly sexual orientation. Secondly, the participant had to indicate to what extent they agreed to statements (using a Likert scale, from 1 till 5, 1 indicating 'strongly disagree' and 5 indicating 'strongly agree'). The first 10 questions related to how involved they are in the queer community now. The second 10 questions related to how involved they were in the queer community 5 years ago. A final 10 questions related to how much social hardship the participant experienced in their youth, based both on a general level and in relation to their sexuality.

To explore the suitability of our data, we used SPSS to perform a statistical analysis regarding the following hypotheses: (1) that queer people would generally score higher on involvement in the queer scene than straight people, (2) that queers would be involved more in the community now than 5 years ago, and finally (3) that hardship would make up for explaining this difference between involvement in the queer community now versus 5 years ago.

By exploring the differences in scores on involvement in the queer scene between queer people and straight people, two of our hypotheses were confirmed: Queer people generally score higher on involvement in the queer scene than straight people, and queers are involved more in the community now than 5 years ago. Another analysis was needed to check the assumption that differences in scores were dependent on the hardship that people experienced by verifying a (possible) a correlation of the scores with the scores on the hardship questions. However, Pearson's correlation r of 0,056 indicated no correlation for the variables. This refutes the hypothesis that the increase in identification with the queer community is mediated by the degree of social hardship experienced when young.

[1] A more detailed account of this section can be requested from the third author.

Next, the empirical data were reshaped in a format compatible with the format of the simulation outcomes so that parameter tuning would provide the best possible solution for the model and the empirical data to fit together. Scenario 3 was chosen for the parameter tuning as it would be the best possible fit for real-life scenarios: as a case where each individual knows each other individual resembles a real-world scenario most. The connection weights for the model were set under the assumption that some segregation was already in place: Straight people were set to a connection weight of 0.8 to other straight people, knowing mostly other straight people and a connection weight of 0.3 to queers. For queers, it was the other way around, setting connection weights to other queers at 0.8 and to straights at 0.3. This leaves some parameters of the model to still be tuned: the speed factor $\boldsymbol{\eta}_X$ for each state X, the steepness $\boldsymbol{\sigma}$ of the alogistic combination function, the threshold $\boldsymbol{\tau}_{\log}$ of the alogistic combination function, the threshold $\boldsymbol{\tau}_{\hom,X,Y}$ of the simple linear homophily, and the amplification factor $\boldsymbol{\alpha}_{X,Y}$ of the simple linear homophily.

The way we estimated these parameters was through exhaustive search. The exhaustive search method is a problem-solving technique in which all possible candidate solutions for parameter values are investigated on how well they make the model fit to the data. Because testing each parameter with a grain size of 0.05 would lead to combinatorial explosion, the way to execute the exhaustive search was by iterative refinement, starting with larger grain sizes, for example, 0.5 or 0.1 (depending on the parameter) and narrowing down the grain sizes until the model fits the empirical data best. Speed factors, steepness, and thresholds were investigated with grain size 0.1, and then in a second phase tuned with a grain size of 0.05; however, amplification was investigated with a grain size of 1 and then further tuned with a grain size of 0.5. The values found are $\sigma = 0.53$, $\tau_{\log} = 0.2$, $\tau_{\hom} = 0.1$, $\alpha = 3.5$, and $\boldsymbol{\eta}_{X_1} = 0.1$, $\boldsymbol{\eta}_{X_2} = 0.1$, $\boldsymbol{\eta}_{X_3} = 0.1$, $\boldsymbol{\eta}_{X_4} = 0.35$, $\boldsymbol{\eta}_{X_5} = 0.3$, $\boldsymbol{\eta}_{X_6} = 0.3$, $\boldsymbol{\eta}_{X_7} = 0.3$, $\boldsymbol{\eta}_{X_8} = 0.3$, $\boldsymbol{\eta}_{X_9} = 0.3$, $\boldsymbol{\eta}_{X_{10}} = 0.3$. Simulation outcomes for the tuned parameters are depicted in Fig. 5. An overview of the remaining errors is shown in Table 5.

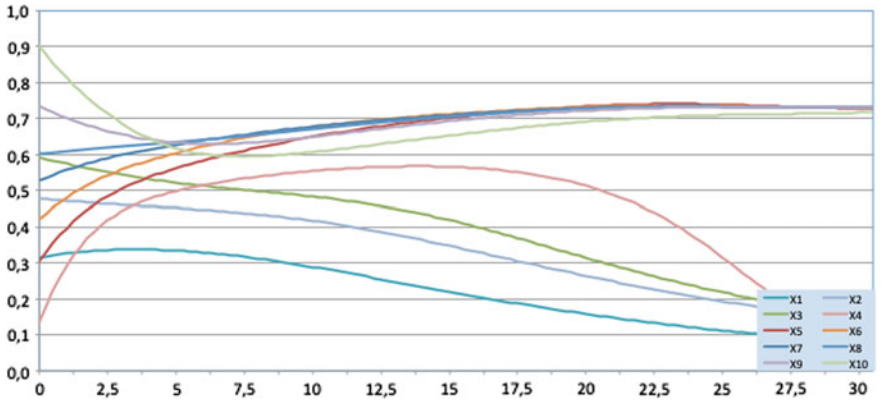

Fig. 5 Simulation modeling of the empirical data. The *X*-axis represents time, and the *Y*-axis represents the identification with the community

Table 5 Calculated error: average absolute deviation and root mean square

State	X_1	X_2	X_3	X_4	X_5	X_6	X_7	X_8	X_9	X_{10}	Total	
Empirical equilibrium	0.357	0.597	0.583	0.601	0.694	0.718	0.778	0.856	0.745	0.88		
Model equilibrium	0	0	0	0	0.747	0.747	0.747	0.747	0.747	0.747		
Absolute deviation	0.357	0.597	0.583	0.601	0.053	0.029	0.031	0.109	0.002	0.133	0.2495	Average deviation
Square of deviation	0.127	0.356	0.340	0.361	0.003	0.001	0.001	0.012	0.000	0.018	1.219	SSR
								Root mean square			0.3492	

Naturally, some variances exist between the proposed model and the empirical data. Using the root mean square to calculate the differences between the values of the model equilibria and equilibria of the empirical data (the final state of involvement in the queer community), this difference should be kept to a minimum in tuning the parameters. The achieved results of the calculated average (absolute) deviation (0.2495) and root mean square (0.3492) are depicted in Table 5, last column.

6 Conclusion

This paper investigated the interplay or co-evolution of the social contagion principle and the homophily principle in their application in an adaptive temporal-causal network model. Both principles were modeled and applied in three model scenarios. State values represented personal convictions, while the connections between states represented real-life social interaction, leading to influencing behavior.

The first scenario used an adaptive normalized scaled sum function to model social contagion. It showed the segregation behavior of a group of ten people into either two or three communities, depending on parameters such as speed factors, threshold factors, and steepness factors. The second scenario used the advanced logistic sum function and showed a separation into two communities that were not entirely defined by the initial grouping of connections. Furthermore, it demonstrated the spiraling of values beyond the range of initial values: a pattern that is not achievable with linear functions such as scaled sum functions. This pattern is sometimes called 'emotion amplification' [3], where emotions or opinions are amplified through sharing them.

The simulation of the third scenario also used the advanced logistic sum function, with the addition of connections to all other nodes in the network. This scenario is slightly more life-like. This scenario showed the segregation into two groups, and the amplifying behavior as discussed in Scenario 2. Furthermore, the third scenario showed a pattern of polarization, in which the values of the two groups increasingly move apart. In social terms, this can be compared to group identification, in which the more the other team disagrees with you, the stronger your opinion gets. It also shows signs of a process called 'othering', in which an individual's or group's identity strongly depends on what they are *not*. These phenomena can be observed in many social situations, with the political system of the USA being a classic example. This process may well contribute to segregating behavior, including political 'echo chamber' that is online social media [12], or the taking shape of subgroups or communities.

The final section of this paper described our attempt to gather empirical data regarding the shaping of the queer community, and the segregating behavior that it relates to. Before using the data in the network model, a statistical analysis showed that there was a significantly higher identification with the queer community of sexual queers than heterosexual participants. It also revealed that queer people had a higher number of queer friends and showed a higher increase in identification with the queer community than heterosexuals. The hypothesis stating that the level

of identification increase is mediated by social hardship experienced in youth was rejected. The empirical data were transformed to fit the model (based on Scenario 3), and an exhaustive search tuning method was performed in order to tune the parameters to best fit the empirical data. The lowest average linear deviation was found to be 0.386. This is relatively high, which can partly be attributed to the fact that the empirical data used an average of scores, leading to values that lie relatively close to one another but are still significantly different. In the model, however, every state represented the average of a group of 5 or 6 people. Moreover, the combination of the advanced logistic sum function and the simple homophily function has a polarizing tendency (as described in Scenario 2), which was not clearly visible in the empirical data.

The current research may be improved by using more than 10 nodes, preferably 50 or more. Not only would this overcome the limitation of having to group participants together and losing their unique trends, but it also might be expected that the interplay between 50 nodes is vastly different from that of 10 nodes, in the way that a classroom with fifty children acts different than one with ten.

Additionally, the empirical data regarding the correlation between youth social hardship and connectedness to the queer community did not show a correlation (or even a trend). This may be due to the survey used, in which only 10 questions were focused on the general social hardship, while a focus on sexuality-related hardship would have been more useful. Secondly, the survey answers are strongly constrained by the snowball effect that was used for gathering the data: Many people who filled in the questionnaire knew others, which results in bias when attempting to study the formation of communities.

Finally, the study would be highly improved if the individual connections between people would be investigated over time. Now, questions about the number of queer people in the individual's network were used to approximate the average effect, while the combination of using the real individual interactions in a network of 50 nodes would give deeper insight into the workings of human group behavior.

Overall this research might be considered as a step in the direction of understanding more about segregation and polarizing behavior. Especially, the adaptiveness, using homophily, is indispensable for the future of creating temporal-causal models of human interactions and their consequences. The work reported here contributes by exploring the use of variants of such network models in the specific real-world context addressed.

References

1. Batson, C.D., Ahmad, N., Tsang, J.-A.: Four motives for community involvement. J. Soc. Issues **5**(8.3), 429–445 (2002)
2. Beemyn, B.: Creating a place for ourselves: lesbian, gay, and bisexual community histories. Routledge (2013)
3. Bosse, T., Duell, R., Memon, Z.A., Treur, J., van der Wal, C.N.: Agent-based modeling of emotion contagion in groups. Cogn. Comput. **7**, 111–136 (2015)

4. Harcourt, J.: Sexual identity distress, social support, and the health of gay, lesbian, and bisexual youth. In: Current issues in lesbian, gay, bisexual, and transgender health, pp. 97–126. Routledge (2013)
5. Holme, P., Newman, M.E.J.: Nonequilibrium phase transition in the coevolution of networks and opinions Phys. Rev. E **74**(5), 056108 (2006)
6. Kuipers, B.J.: Commonsense reasoning about causality: deriving behavior from structure. Artif. Intell. **24**, 169–203 (1984)
7. Kuipers, B.J., Kassirer, J.P.: How to discover a knowledge representation for causal reasoning by studying an expert physician. In: Proceedings Eighth International Joint Conference on Artificial Intelligence, IJCAI'83, Karlsruhe. William Kaufman, Los Altos, CA (1983)
8. McPherson, M., Smith-Lovin, L., Cook, J.M.: Birds of a feather: homophily in social networks. Ann. Rev. Soc. **27**(1), 415–444 (2001)
9. Meyer, I.H.: Minority stress and mental health in gay men. J. Health Soc. Behav. **36**, 38–56 (1995)
10. Meyer, I.H.: Prejudice, social stress, and mental health in lesbian, gay, and bisexual populations: conceptual issues and research evidence. Psychol. Sex. Orient. Gend. Diversity **1**(S), 3–26 (2013)
11. Pearl, J.: Causality. Cambridge University Press (2000)
12. Sunstein, C.R.: # Republic: Divided Democracy in the Age of Social Media. Princeton University Press (2018)
13. Treur, J.: Dynamic modeling based on a temporal–causal network modeling approach. Biol. Inspired Cogn. Archit. **16**, 131–168 (2016)
14. Treur, J.: Network-Oriented Modeling: Addressing Complexity of Cognitive, Affective and Social Interactions. Springer, Cham (2016)
15. Treur, J.: Relating emerging network behaviour to network structure. In: Proceedings of the 7th International Conference on Complex Networks and their Applications, Complex Networks'18, vol. 1. Studies in Computational Intelligence, vol. 812, pp. 619–634. Springer (2018a)
16. Treur, J.: Relating an adaptive social network's structure to its emerging behaviour based on homophily. In: Proceedings of the 7th International Conference on Complex Networks and their Applications, Complex Networks'18, vol. 2. Studies in Computational Intelligence, vol. 813, pp. 341–356. Springer (2018b)
17. Treur, J.: The ins and outs of network-oriented modeling: from biological networks and mental networks to social networks and beyond. Trans. Comput. Collect. Intell. **32**, 120–139. Based on Keynote Lecture at the 10th International Conference on Computational Collective Intelligence, ICCCI'18 (2019)
18. Vazquez, F.: Opinion dynamics on coevolving networks. In: Mukherjee, A., Choudhury, M., Peruani, F., Ganguly, N., Mitra, B.: (eds.) Dynamics on and of Complex Networks, vol. 2, Modeling and Simulation in Science, Engineering and Technology, pp. 89–107. Springer, New York (2013)